ULTRASOUND PROPAGATION IN FRACTURES WITH INTRAMEDULLARY NAILING

F. Catelani*, A. J. F. Pereira*, C. B. Machado**, C. P. Carvalho*, P. T. C. R. Rosa*, D. P. Oliveira***, M. A. von Krüger* and W. C. A. Pereira*

*Biomedical Engineering Program – COPPE/UFRJ, Rio de Janeiro, Brazil
**Biomedical Ultrasound Laboratory – Estácio de Sá University, Rio de Janeiro, Brazil
***National Institute of Metrology, Quality and Technology – INMETRO, Rio de Janeiro, Brazil
email: fernanda.catelani@peb.ufrj.br

Abstract: Studies on ultrasound (US) propagation in bone tissue have been conducted in view of its ability to stimulate the consolidation process for normal or pathological fracture. However, the action mechanisms of ultrasound, as well as its propagation modes in bone, are still not completely understood. This study evaluated the parameters Integrated Reflection Coefficient (IRC), the Frequency Slope Integrated Reflection (FSIR) and Sound Pressure Level (SPL) through a pulse-echo propagation in a phantom of cortical bone and through 2D computational simulation, including five transverse fracture gaps (0, 1, 2, 3 and 4 mm) with and without the presence of an intramedullary nailing (IN). The results showed a correlation between IRC and SPL and these with the size of the fracture and the echoes of the evaluated interfaces, while FSIR helped to identify the presence of IN in combination with other parameters. The simulations followed the trend of the experimental results. It was concluded that the evaluated parameters contributed to the mechanical characterization of the phantom bone conditions evaluated, and points to the achievement of future experiments that include other frequency of ultrasound for analysis of backscatter.
Keywords: Ultrasound, pulse-echo, fracture, intramedullary nailing, simulation.

Introduction

Ultrasound (US) is a mechanical wave which, during propagation in a medium, interacts with its properties [1]. US equipment is relative simple to use and produce a non-ionizing wave, being widely applied in health domain for diagnostics and therapy, including for bone tissue [2]. Bone is an anisotropic tissue that benefits from low-intensity pulsed ultrasound stimulation (LIPUS), used in fractures and nonunions to accelerate tissue regeneration [3]. In some types of fractures, medical doctors chose to use intramedullary nailing (IN) to increase diaphyseal stability of bone fragments, however, in certain cases, IN can disturb endosteal blood flow or, in the case of radiation with US, increase local energy absorption [4,5], which can delay the consolidation process [6].

Although the well-established benefits [2], literature is still not clear about the mechanisms of propagation of US in bone [2,7]. For that reason, quantitative ultrasound (QUS) has been proposed to help researcher in the understanding of how US waves travel through bone tissue [8,9]. QUS principles are applied in numerical simulations, simplifying structure analysis [10,11] and in experiments with animal models or bone-mimicking phantoms [12,13].

Therefore, the aim of this study was to characterize US propagation (with a pulse-echo setup) in fractures with and without IN, comparing the results of an experimental model using bone phantom with two-dimensional (2D) numerical simulations.

Materials and methods

Experimental protocol – QUS analysis was performed by means of a pulse-echo setup in a degassed water tank at 25.1 ± 0.5°C. An emitter-receiver transducer with nominal frequency of 1 MHz (Olympus® Panametrics, model V-303-SU), diameter of 14.4 mm and focal distance of 5.1 mm, was posiotioned perpendicularly at 11.3 mm to the greater axis of the sample (Figure 1), composed of epoxy-made cylindrical bone phantoms (Sawbones®), with diameter 24.8 mm and cortical thickness 5.9 mm (Figure 2).

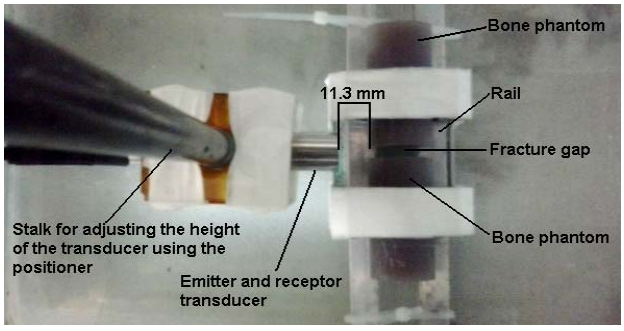

Figure 1: Superior view of the experimental apparatus.

US signals were collected with a continuous phantom and with two pieces, side by side, to simulate five transverse fracture sizes (gaps of 0, 1, 2, 3 and 4 mm). Signals were collected with and without the cylindrical nailing made of austenitic stainless steel 304, diameter of 13 mm, inside the medullar canal, simulating IN. Fracture gaps were made with the aid of

plates and rectangular shaft.

Before each experiment, the transducer was positioned according to the greater echo obtained in the interface water-phantom (0 mm). The positioning was verified by observing signal amplitudes during transducer displacement, parallel to the phantom, until 3 mm under and above the initial position, using a linear 3-axis positioner (Newport®) (Figure 2-D). For the reference signal, the phantom was substituted by a ideal reflector of stainless steel.

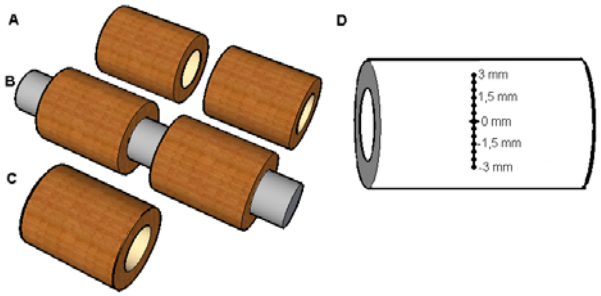

Figure 2: Cylindrical bone phantom models with fracture and without IN (A), with fracture and IN (B) and an integer bone phantom (C). In (D) it can be observed the transducer displacement in relation to the phantom.

Signal generation and acquisitions – The transducer was excited by a SR9000 (Matec®) board and the echos were visualized on a digital oscilloscope (Tektronix® TDS 2024B). Signals were saved in a computer by a program in Labview (National Instruments®).

2D simulations – Simulations were run using SimSonic2D, which uses a time-domain finite element method [14] based on Virieux discretization scheme. The numerical model of the propagation medium was developed in Matlab (MathWorks® R2007a v. 7.4), with spatial resolution 0.05 mm. The model presented a horizontal and vertical length of 30 mm and 41.25 mm, respectively, and the same thicknesses of the experimental structures. For the pulse-echo transmission, a receptor was positioned at the same side of the emitter, also with the same dimensions.

Simulations considered bone as a isotropic material, and it was used the stiffness matrix (C_{11}, C_{22}, C_{12}, C_{33}) and density values found in literature (water = 1 g/cm^3; bone = 1,92 g/cm^3 and steel 304 = 8 g/cm^3). It were generated 9 signals with duration 50 µs without absorption.

Parameters for analysis – It were evaluated the Integrated Reflection Coefficient (*IRC*) [2,15,16]; the Frequency Slope Integrated Reflection (*FSIR*) [17]; and the Sound Pressure Level (*SPL*) [18,19].

The *IRC* was obtained with the reflection echoes power spectra from phantom ($P_{phantom}$) and reference ($P_{reference}$), using the Apparent Backscatter Transfer Function (*ABTF*), showed in Equation 1 [16].

$$ABTF = 10\log_{10} P_{phantom}(f) - 10\log_{10} P_{reference}(f) \quad (1)$$

The *IRC* [15,17,20] assessed the acoustic impedance in interface 1 (water-phantom) and interface 2 (phantom-medullar canal component, being water or metal), using Equation 2.

$$IRC = \frac{\int_{f\min}^{f\max} [ABTF] \cdot df}{f_{\max} - f_{\min}} \quad (2)$$

The *FSIR* was found using a linear regression of *ABTF versus* frequency [17]. The *SPL* was estimated by the traditional method, using the maximum amplitude of the echo on each interface [11,13].

Signal processing and analysis – Reference and phantom signals were processed in Matlab®. The sampling frequency of experimental and simulation signals were 25 MHz and 314 MHz, respectively. The selection of reference echoes as well as from each interface was performed by creating a temporal window (experimental case) with the same excitation pulse length (4 µs), while for the simulation case it was detected the first signal arrived in the receptor (2,99 µs). Widows were centered in relation to the amplitude peak of each signal (Figure 3).

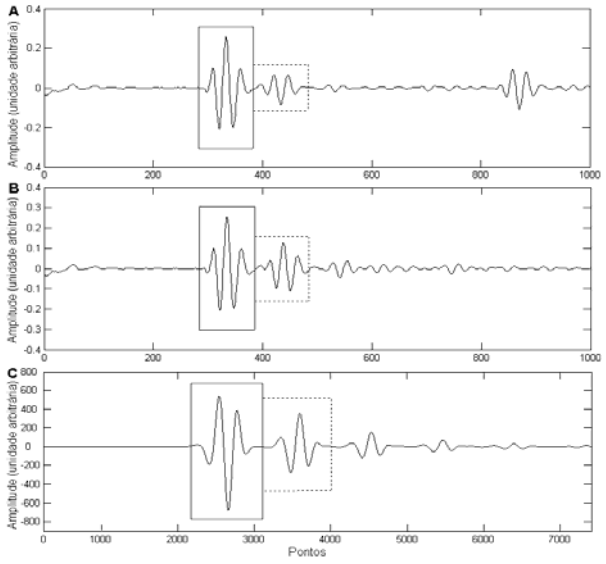

Figure 3: Phantom signal without (A) and with IN (B); and the simulation signal without IN (C). The windowed signal on interface 1 (water-phantom) with a continuous line and on interface 2 (*phantom*-medular canal component) with dashed line.

Statistics – Experimental values did not follow a normal distribution (Kolmogorov-Smirnov test). Therefore it was performed a non parametric test (Friedman test) to compare all fractures, followed by a *post hoc* Wilcoxon test for two paired samples. This test was also used to compare samples with and without IN

and between interfaces of the same signal. The Spearman coefficient was obtained to correlate: both interfaces at the same fracture; *IRC* and *FSIR* and each of them with the *SPL*. Finally, the Mann Whitney U test was applied for independent samples to compare experimental and simulation results.

For all tests, a significance level of 0.05 (except for *post hoc* test which, after Bonferroni correction, considered 0.005). The software SPSS Statistics (IBM® v. 20.0) was used for the statistical analysis.

Results

With respect to transducer positioning, greater values of *SPL* were obtained for dislocations of the transducer between 0 and 1 mm (Figure 2-D).

The Friedman test showed similar values for *FSIR* on fractures of interface 1. The *post hoc* Wilcoxon test showed that differences of FSIR for interface 2 increased with the presence of IN. Table 1 presents the median values of experimental results.

Comparing fractures with and without IN, there was similarity in only two fracture sizes for *IRC* and *SPL* and in three sizes when analyzing *FSIR* from interface 1. On interface 2, however, only *FSIR* presented similarity, nevertheless only for two fracture sizes. When both interfaces are compared from the same signal, similarity was observed only for *FSIR* from fracture 1 mm without IN.

Table 1: experimental median values of *IRC*, *FSIR* and *SPL*, without (IN_0) and with (IN_1) intramedullary nailing.

	Interface 1		**Interface 2**	
Fractures	*IRC* (dB)			
(mm)	IN_0	IN_1	IN_0	IN_1
0	-5.2	-4.9	-16.1	-12.4
1	-6.1	-5.5	-20.9	-17.0
2	-7.3	-7.5	-21.8	-20.8
3	-9.6	-8.5	-23.9	-20.8
4	-11.7	-10.9	-28.6	-25.2
	FSIR (dB·MHz^{-1})			
	IN_0	IN_1	IN_0	IN_1
0	1.6	-2.3	-4.4	-4.2
1	-2.1	-2.6	1.6	2.5
2	-1.9	-2.1	-4.9	-4.4
3	-2.0	-1.7	-5.3	0.6
4	-1.9	-1.8	-9.7	-0.1
	SPL (dB)			
	IN_0	IN_1	IN_0	IN_1
0	-9.6	-8.8	-38.5	-25.8
1	-11.7	-10.4	-48.1	-36.6
2	-14.8	-15.2	-50.9	-46.7
3	-19.8	-17.4	-54.1	-48.1
4	-24.8	-23.3	-62.9	-58.1

Analyzing *IRC* and *FSIR* on interface 1, without IN, Spearman coefficient showed good correlation ($\rho < -0.85$) for fractures from 0 to 3 mm and on interface 2 the coefficient became positive among fractures 1, 2 and 4 mm. With the presence of IN there was a reduction in correlation between *IRC* and *FSIR* limited for two fracture sizes.

SPL presented high correlation with *IRC* ($\rho > 0.90$), independent of the fracture size, interfaces or presence of IN, situation which did not occurred with *FSIR*. When interfaces of a specific fracture were compared, it was also observed a high correlation for *IRC* ($\rho > 0.94$) and *SPL* from interfaces ($\rho > 0.92$).

When comparing medians from experimental parameters with the results from simulations, there was a significant difference among all the parameters, except for FSIR values without IN. Simulations presented higher values than experimental IRC and SPL values. These parameters also reduced with the increasing in fracture length, which was more accentuated on interface 2 (Table 2).

Table 2: simulation values of *IRC*, *FSIR* and *SPL*, without (IN_0) and with (IN_1) intramedullary nailing.

	Interface 1		**Interface 2**	
Fractures	*IRC* (dB)			
(mm)	IN_0	IN_1	IN_0	IN_1
0	-2.9	-2.9	-8.6	-8.0
1	-3.6	-3.6	-10.3	-10
2	-4.3	-4.3	-11.3	-11
3	-5.1	-5.1	-12.4	-12
4	-6.0	-5.9	-13.8	-13.3
	FSIR (dB·MHz^{-1})			
	IN_0	IN_1	IN_0	IN_1
0	0	0	0.1	0.1
1	0.1	0.1	0.8	1.2
2	0.1	0.1	0.6	1.0
3	-0.1	-0.1	1.0	0.7
4	-0.3	-0.3	1.1	0.9
	SPL (dB)			
	IN_0	IN_1	IN_0	IN_1
0	-6.6	-6.7	-15.2	-18.8
1	-8.3	-8.3	-19.0	-23.1
2	-10.0	-10.0	-21.3	-25.3
3	-12.0	-12.0	-23.8	-27.9
4	-14.0	-14.0	-27.0	-30.4

Discussion

The present work used an experimental and numerical model considering bone and IN diameter compatible to the human fêmur [21]. The frequency of 1 MHz was capable of providing data from both cortical sides, when IN was absent.

The transducer positioning, considering the greater reflected amplitude on interface 1 (0 mm), was intended to be the point of greater phantom convexity (Figure 2-D). The *SPL* showed that this position was closer than the desired point with a dislocation error up to 1 mm in relation to the point of greater reflection.

The *IRC* [17,20] estimates the reflection quantity of a tissue and it was applied by Hakulinen et al. [15] who

verified the great relation of this parameter, in association with sound velocity (SOS), to predict volumetric bone mineral density (BMD_{vol}) and the mechanical properties of *in vitro* bovine trabecular bone, however it was not observed correlation between *IRC* and the normalized attenuation (nBUA in dB/MHz/cm), and between *IRC* and mechanical properties of bone. The authors stated that it was due to the high density of bovine bone compared to human bones, which were better evaluated by the same parameter [22].

Different from the work of Hakulinen et al. [15], in the present study found a positive correlation between *IRC* and *SPL*, which was already expected due to the inversely proportional relation between reflection and attenuation, the latter caused by backscattering. The increase in *SPL* with the reduction of fracture length corroborated results in literature, which associates the lower attenuation to the final stages of bone healing, even in *in vivo* experiments [19]. In this case, the reduction in the phantom spacing mimicked the consolidation process [12].

Studies with *in vivo* rat femur diaphysis with US frequency of 5 MHz found average values of *IRC* of approximately -28 dB [17], from -4.8 to -22.4 dB [23] and -27.5 ± 2.01 dB [20]. Another work evaluated the human trabecular bone at the distal femoral epiphysis and proximal tibia [11] verifying a variation of *IRC* with frequency from 0.5 to 5 MHz, obtaining a higher value of -10.0 ± 3.8 dB. Hakulinen et al. [15] applied US in the range of 0.2 to 0.6 MHz observing mean values from -4.9 to -27.2 dB in the head and greater trochanter of bovine femur, respectively. The *IRC* values found in literature were within the range found in the present study, although some variation may be due to the bone type, if human or not, if cancellous or cortical bone, for example, and also to the frequency applied in the acquisition. Moreover, this work considered fractures with and without IN. The negative values of *IRC* showed that the greater amplitudes of reflection were associated to the lower wave frequencies.

According to Pereira et al. [17], *FSIR* represents a fraction of the reflection correspondent to each analyzed frequency and it is related to the cortical density, which may provide usable information about bone healing, together with *IRC*. These authors found *FSIR* varying from -5.29 to 3.2 $dB \cdot MHz^{-1}$, reaching positive and negative values, a similar result from the present study. They also observed a positive correlation between *IRC* and *FSIR* with the superficial BMD, verified with quantitative computerized tomography. The *FSIR,* however, presented variation, between each experiment, greater than the expected, showing similar results with the present work, inversely *IRC* and *SPL* presented a more homogeneous distribution than *FSIR*, which enabled the differentiation of interfaces and fractures.

IRC is a promising parameter to be assessed in pulse-echo approaches, since its estimation is not dependent of tissue thickness, different from SOS estimation. It could be applied to several body regions, contributing to the study of fractures and bone healing, mainly when the cortical shell is evaluated, since attenuation produced by soft tissues would have a smaller influence, not affecting *IRC* and backscattering measures in trabecular bone [15].

For the identification of IN, the results showed that a combination of the three parameters would be ideal. The IN led *IRC* and *SPL* values to be more positive, meaning a greater acoustic impedance and a lower wave attenuation, respectively, increasing energy concentration, outcome verified with the root mean square applied in previous studies in 2D simulations with reamed and non-reamed IN [4,5].

Hakulinen et al. [11] also coupled experimental and 2D simulation results showing the viability of these studies. Nevertheless, they stated that it has to be taken into consideration the limitations of this work, because bone is an anisotropic material. The high values of *SPL* and *IRC* found in simulations can be attributed to the neglected absorption, resulting on an increase of the power spectra from simulation echoes, not influencing *FSIR*.

The present work had some drawbacks like the use of cylindrical phantoms diverging from the human femoral diaphysis morphology. However, as it could be seen, it was possible to obtain results which corroborate literature findings [17,20,23].

These findings were important to the experimental and simulation characterization of transverse fracture models with and without IN, using reflection and attenuation US parameters. Further research point out to new experiments using higher US frequencies, leading to the assessment of backscattering parameters, and the utilization of bone phantoms with a more realistic morphology and composition.

Acknowlegments

To CNPq, CAPES and FAPERJ for financial support and to DSc student José Francisco Silva Costa Júnior for experimental support.

References

[1] Fish P. Physics and instrumentation of diagnosis medical ultrasound. England: John Wiley and Sons; 1999.

[2] Romano CL, Romano D, Logoluso N. Low-intensity pulsed ultrasound for the treatment of bone delayed union or nonunion: a review. Ultras Med Biol 2009; 35(4): 529-36.

[3] Huber M, Prant L, Gehmert S. Successful treatment of nonunion in severe finger injury with low-intensity pulsed ultrasound (LIPUS): a case report. J Med Cas Rep. 2012, 6(1): 1-3.

[4] Catelani F, Ribeiro APM, Melo CAV, Pereira WC, Machado CB. Ultrasound propagation through bone fractures with reamed intramedullary nailing: results from numerical simulations. Proceedings of Meetings on Acoustics; 2013 Jun 2-7; Montreal, Canada. 2013. p. 1-8.

[5] Catelani F, Ribeiro APM, Melo CAV, Machado CB, Pereira WCA. Propagação do ultrassom em fraturas com haste intramedular não fresada usando simulação em 2D. Proceedings of XXIII Congresso Brasileiro de Engenharia Biomédica; 2012 Out 2-5; Recife, Brasil. 2012. p. 2332-36.
[6] Larsen LB, Madsen, JE, Høiness, PR, Øvre, S. Should insertion of intramedullary nails for tibial fractures be with or without reaming? J Orthop Trauma. 2004, 18(3): 144-49.
[7] Snyder BM, Conley J, Koval KJ. Does low-intensity pulsed ultrasound reduce time to fracture healing? A meta-analysis. The Am J Orthop. 2012; 41(2): E12-E19.
[8] Axelrad TW, Einhorn TA. Use of clinical assessment tools in the evaluation of fracture healing. Injury-int J Care of the Injured. 2011. 42: 301-5.
[9] Machado CB. Ultrasound in Bone Fractures: from Assessment to Therapy. New York: Nova Science Publishers, Inc., 2013.
[10] Kaufman GL, Siffert RS. Ultrasound simulation in bone. IEEE T Ultras Fer Freq Contr 2008. 55: 1205-18.
[11] Hakulinen MA, Day JS, Töyräs J, Weinans H, Jurvelin J.S. Ultrasonic characterization of human trabecular bone microstructure. Phys Med Biol 2006. 51(6): 1633-48.
[12] Njeah CF, Kearton JR, Boivin CM. The use of quantitative ultrasound to monitor fracture healing: feasibility study using phantoms. Med Eng Phys. 1998. 20: 781-86.
[13] Machado CB, Pereira WC, Granke M, Talmant M, Padilla F, Laugier P. Experimental and simulation results on the effect of cortical bone mineralization in ultrasound axial transmission measurements: a model for fracture healing ultrasound monitoring. Bone. 2011. 48: 1202-9.
[14] Bossy E, Talmant M, Laugier P. Three-dimensional simulations of ultrasonic axial transmission velocity measurement on cortical bone models. J Acoust Soc Am. 2004, 115(5): 2314-24.
[15] Hakulinen MA, Töyräs J, Saarakala S, Hirvonen J, Kröger H, Jurvelin JS. Ability of ultrasound backscattering to predict mechanical properties of bovine trabecular bone. Ultras Med Biol.2004. 30(7): 919-27.
[16] Hoffmeister BK, Johnson DP, Janeski JA, Keedy DA, Steinert BW, Viano AM, Kaste SC. Ultrasonic characterization of human cancellous bone in vitro using three different apparent backscatter parameters in the frequency range 0.6-15.0 MHz. IEEE Trans Ultras Freq Control. 2008. 55(7): 1442-52.
[17] Pereira AJF, Costa TCFV, Schanaider A, Krüger MAV, Pereira WCA. In vivo characterization of long-bone in animal model by ultrasonic reflection parameters: IRC and FSIR. Proceedings of the Pan American Health Care Exchanges; 2012 Mar 26-31; Miami, USA. 2012. p. 106-10.
[18] Hoffmeister BK, Holt AP, Kaste SC. Effect of the cortex on ultrasonic backscatter measurements of cancellous bone. Phys Med Biol. 2011. 56(19):6243–55.
[19] Barbieri G, Barbieri CH, Matos PS, Pelá CA, Mazzer N. Estudo comparativo da velocidade e atenuação ultra-sônica na avaliação da consolidação óssea. Acta Ortopédica Brasileira. 2009. 17(5): 273-8.
[20] Matusin DP, Pereira AJF, Machado CB, Ferreira ML, Schanaider A, Pereira WCA. Caracterização ultrassônica *in vivo* de osso longo em modelo animal. Proceedings of XXII Congresso Brasileiro de Engenharia Biomédica; 2010 Nov 21-25; Tiradentes, Brasil. 2010. p. 627-30.
[21] Huang BW, Chang FS, Lin AD, Tsai YC, Huang MY, Tseng JG. Dynamic characteristics of a hollow femur. Life Science Journal. 2012. 9(1): 723-726.
[22] Han S, Rho J, Medige J, Ziv I. Ultrasound velocity and broadband attenuation over a wide range of bone mineral density. Osteoporosis Int. 1996. 6(4): 291-6.
[23] Fontes-Pereira DP, Matusin PR, Schanaider A, Krüger MAV, Pereira WCA. Ultrasound method applied to characterize healthy femoral diaphysis of Wistar rats in vivo. Braz J Med Biol Res. 2014. 47(5):403-10.